RSC Advances

PAPER

View Article Online
View Journal | View Issue

Cite this: RSC Adv., 2015, 5, 86885

Facile preparation of rare-earth semiconductor nanocrystals and tuning of their dimensionalities†

Hechun Lin,‡[a] Qianqian Luo,‡[a] Wen-Yi Tong,[a] Chunli Jiang,[a] Rong Huang,[a] Hui Peng,*[ab] Lai-Chang Zhang,[c] Jadranka Travas-Sejdic[b] and Chun-Gang Duan[a]

Received 29th August 2015
Accepted 9th October 2015

DOI: 10.1039/c5ra17506b

www.rsc.org/advances

EuS and Gd_2O_2S nanocrystals with narrow size distribution are synthesized in high yields by the thermal decomposition of Eu(oleate)$_3$ or Gd(oleate)$_3$ in oleylamine using CS_2 as the sulfur source. The dimensionalities of these nanocrystals can be facilely tuned by the addition of 1-dodecanethiol. The morphologies and crystal structures of EuS and Gd_2O_2S nanocrystals are characterized by TEM and XRD. The magnetic properties of the obtained nanocrystals are also investigated. The experimental results illustrate that CS_2 is an effective sulfur source for the preparation of metal sulfide and lanthanide oxysulfide semiconductor nanocrystals.

Introduction

The rare-earth containing semiconductors, which have been studied extensively since the 1960s,[1,2] have attracted renewed interest due to their remarkable semiconducting and magnetic properties. Among the rare-earth containing semiconductors, EuS and Gd_2O_2S receive special attention. Because the pronounced ferromagnetism of EuS provides spin-polarized electrons which induce promising applications in spin-filter devices as the tunnel barriers.[3,4] Furthermore, enhanced Curie temperature of EuS *via* hydrostatic pressure,[5,6] epitaxial strain,[7] or electrons injecting with other rare-earth ions such as Tb,[8] and Gd,[9] promotes the possibility of EuS to be applied for semiconductor-based next-generation spintronic devices. Gd_2O_2S is known as a wide-gap material with high chemical stability and high thermal stability. Rare earth ion activated Gd_2O_2S materials show greatly potential applications in various fields, such as field emission displays, long lasting phosphorescence and bioimaging.[10,11]

The novel size-dependent properties displayed by semiconductor nanocrystals have initiated the current worldwide intense research on nanomaterials, especially the ones with magnetism. It is reported that magnetic properties such as tunnelling magnetoresistances[12] and magnetic moments[13] can be easily modulated in nanostructured materials. More interestingly, size-dependent magnetism[14,15] and size-dependent optics[16] of EuS nanomaterials have been suggested in addition to the increasing number of outstanding properties observed in bulk EuS. Now, research interests have been expanded into controllable synthesis of nanomaterials with the desired dimensionality and also in understanding the correlations between the dimensionalities and their properties.

Enormous efforts have been devoted to synthesizing EuS and Gd_2O_2S nanocrystals. In order to get monodispersed nanocrystals, sulfur source is one of critical points of experimental conditions, especially in the case of Gd_2O_2S. The theory of hard and soft acids and bases (HSAB) predicts a lack of affinity between the hard Lewis acid Gd^{3+} and the soft Lewis base S^{2-}.[17] In practice, this theoretical bottleneck is expressed as the lack of an effective sulfurization method in preparing Gd_2O_2S nanocrystals. Reaction of europium metal with thiourea in liquid ammonia under a N_2 atmosphere,[18] thermal decomposed single molecule precursors,[14,15,19–21] as well as liquid phase thermolysis of Eu(oleate)$_3$ and diethylammonium diethyldiocarbamate in the presence of 1-dodecanethiol and phenanthroline[16] have been proved to synthesize EuS nanocrystals. In the case of Gd_2O_2S nanocrystals, thermal decomposed single molecule precursors,[22] combustion[23] and reaction of hydroxycarbonate precursor with urea followed by sulfuration in a H_2S/Ar atmosphere at 750 °C (ref. 24) are reported. However, due to various limitations in the reported methods, such as rigorous reaction conditions resulting in aggregates of particles, the cost of precursors, aggregations, special instrument requirements, or time-consuming in production, it is still of great significance to develop effective synthetic methods to produce these two nanocrystals with facile tuning of the dimensionality.

Here we report a low cost, facile synthesis of EuS and Gd_2O_2S nanocrystals using CS_2 as the sulfur source with the advantages of high-efficiency, and large-scale production. The shape of EuS can be easily tuned from nanocube (3-D) to nanodot (0-D) by the

[a]Key Laboratory of Polar Materials and Devices, Ministry of Education, East China Normal University, Shanghai, China

[b]School of Chemical Science, The University of Auckland, Auckland, New Zealand. E-mail: h.peng@auckland.ac.nz

[c]School of Engineering, Edith Cowan University, 270 Joondalup Drive, Joondalup, Perth, WA 6027, Australia

† Electronic supplementary information (ESI) available: The TEM of EuS-up-scale and synthesis of ZnS, PbS and CdS nanodots. See DOI: 10.1039/c5ra17506b

‡ These authors contributed equally.

addition of 1-dodecanethiol as a surfactant. Similarly, the shape of Gd_2O_2S can be easily tuned from nanodots (0-D) to nanorod (1-D) by the addition of 1-dodecanethiol as a surfactant. The magnetic properties of the obtained EuS nanocrystals and Gd_2O_2S nanocrystals were investigated. It was found that the EuS nanocrystals exhibited strong ferromagnetic property, and the Gd_2O_2S nanocrystals presented paramagnetic property. Additionally, we also illustrates that CS_2 can be used as a cheap and efficient sulfur source for the preparation of other monodispersed metal sulfide, such as CdS, PbS, and ZnS nanocrystals.

Experimental

Materials

All of the reagents used herein were of analytical grade and used as received without any further purification. Oleylamine (mass concentration: 80–90%), 1-dodecanethiol (DT), sodium oleate, $Gd(NO_3)_3 \cdot 6H_2O$ were purchased from Aladdin Industrial Corporation. $EuCl_3 \cdot 6H_2O$ was received from Sigma-Aldrich.

Synthesis of EuS nanocubes (NCs) and nanodots (NDs)

For the synthesis of EuS NCs, $Eu(oleate)_3$ was first prepared according to the literature.[25] $Eu(oleate)_3$ (332 mg) was dissolved in oleylamine (4 mL) under N_2. The solution was heated up to 280–310 °C. CS_2 (0.3 mL) was drop-wise added within 5 minutes with a controlled speed to avoid explosive boiling. The addition of CS_2 quickly led to the color change of the reaction solution from orange to purple, which indicated the formation of EuS. After reacting for half an hour, the mixture was cooled down to room temperature and dispersed to toluene. The purple-black product was collected *via* centrifugation and washed for 4 times with the mixture of toluene and ethanol (1 : 1 in volume). After dried in vacuum oven, 55 mg of final product was obtained. The same procedure was applied for the up-scale synthesis of EuS NCs. 3.32 g of $Eu(oleate)_3$ in oleylamine (40 mL) was used and 0.57 g of final product was obtained. This sample was named as EuS-up-scale.

The synthesis of EuS NDs was similar to the above procedure, except that 1 mL of 1-dodecanthiol was added and the reaction time was 2 hours.

Synthesis of Gd_2O_2S nanodots (NDs) and nanorods (NRs)

The synthesis of Gd_2O_2S NDs is similar to that of EuS NCs. In brief, $Gd(oleate)_3$ was first prepared according to the literature.[26] 334 mg of $Gd(oleate)_3$ was dissolved in oleylamine (4 mL) under N_2. The solution was heated up to 280–310 °C, and CS_2 (0.3 mL) was drop-wise added within 5 minutes. After reacting for 6 hours, the reaction mixture was dispersed to toluene, and the products were collected *via* centrifugation and washed for 4 times with the mixture of toluene and ethanol (1 : 1 in volume). After dried in vacuum oven, 58 mg of orange-brown product was obtained. The synthesis of Gd_2O_2S NRs was similar to that of Gd_2O_2S NDs with the addition of 1 mL of 1-dodecanethiol and the reaction time was 10 hours.

Characterization of nanocrystals

Nanocrystals were characterized by transmission electron microscopy (TEM) and X-ray diffraction (XRD). TEM images were obtained by using a JEM-3010 electron microscope. XRD patterns were collected on a Brucker AXS D8 powder diffractometer unit by using Cu Kα radiation ($\lambda = 0.154$ nm) operating at 40 kV and 40 mA. The patterns were recorded from 20° to 80° in 2θ with a 2θ scan step size of 0.02°. XPS experiments were carried out in a RBD upgraded PHI-5000C ESCA system (Perkin Elmer) with Mg Kα radiation ($h\nu = 1253.6$ eV) or Al Kα radiation ($h\nu = 1486.6$ eV). The magnetic properties of EuS nanocrystals were measured by using a physical property measurement system (Quantum Design PPMS-9, San Diego, USA).

Results and discussion

Morphologies and crystal structure of EuS nanocrystals

The morphology of EuS nanocrystals prepared *via* thermal decomposition of $Eu(oleate)_3$ by using CS_2 as a sulfur source

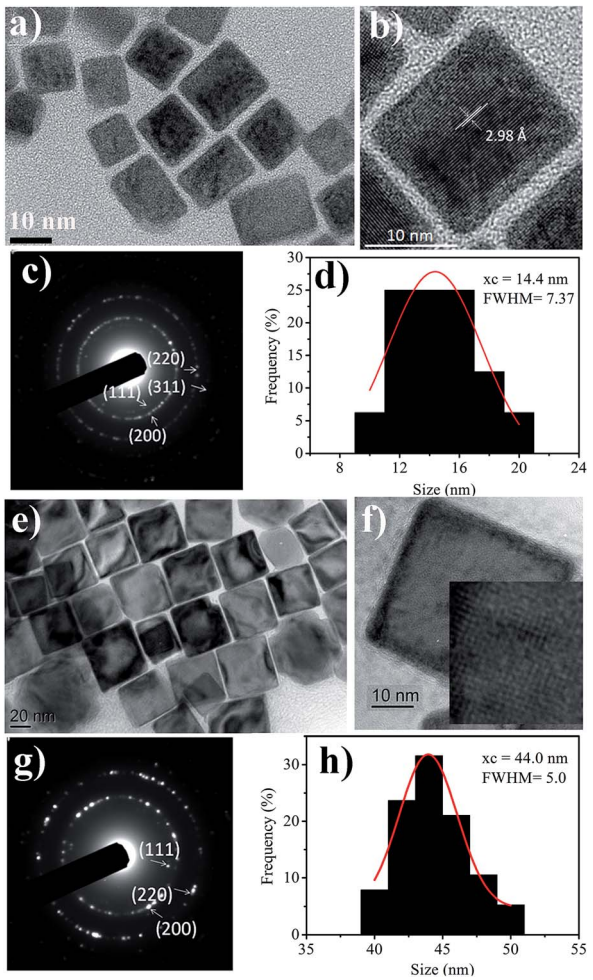

Fig. 1 TEM images of EuS NCs prepared with the reaction time of (a) 0.5 hour and (e) 1 hour. (b) and (f) are corresponding high resolution TEM images. (c) and (g) are corresponding the selected area electron diffraction (SAED) patterns. (d) and (h) are corresponding size histograms.

was first investigated by TEM, as shown in Fig. 1a. It is clear that the obtained EuS nanocrystals are cubic with a size of 10 nm to 20 nm (Fig. 1d). The EuS NCs show clear lattice-fringe profiles in the high resolution TEM image and the lattice spacing is 2.98 Å, which corresponds to the (200) plane (Fig. 1b). These lattice planes are further confirmed by the electron diffraction rings (Fig. 1c). Prolonging the reaction time to 2 hours led to the growth of EuS NCs and the narrow size distribution, as shown in Fig. 1e and h. The average size of obtained EuS NCs is 44 nm. However, the crystals present a little bit surface disorder as show in the high resolution TEM image (Fig. 1f). The crystal structures of obtained EuS NCs were further characterized by XRD. The results are represented in Fig. 2. Diffraction peaks at 25.8, 30.0, 42.8, 50.8, 53.1, 62.2, and 70.6° are assigned (111), (200), (220), (222), (400), (420), and (422) of NaCl type EuS, respectively.

In order to tune the dimensionality of EuS nanocrystals, 1-dodecanethiol was used as a surfactant under the same experimental conditions. The TEM images of obtained EuS nanocrystals are given in Fig. 3. It is clear that the obtained EuS are nanodots, which have a narrow size distribution with the average size of 7.5 nm (Fig. 3d). The lattice fringe of EuS NDs can be clearly seen and the lattice spacing is also 2.98 Å corresponding to (200) plane (Fig. 3b). The XRD profiles of EuS NDs are similar to those of EuS NCs, as shown in Fig. 2. The diffraction peaks are broad and weak because of the small size of EuS NDs. Due to the presence of 1-dodecanethiol which possibly suppresses the anisotropic growth of EuS nanocrystals, the shape of these nanocrystals can be facilely tuned from cube to dot.

Furthermore, a ten-times-scale synthesis of EuS NCs was carried out to investigate the possibility of our method for the large-scale synthesis in practice. A production of 0.58 g EuS NCs in one pot was achieved, which is much larger than previous reported methods.[14,15,19–21] The XRD (Fig. 2) and TEM (Fig. S1 in ESI†) results well demonstrate the potential application for the large-scale synthesis of EuS NCs.

Additionally, monodispersed CdS, PbS, and ZnS nanodots have also been successfully prepared by using the suggested reaction system (the experimental details and results are given in ESI†), which clearly illustrates the generalization of the suggested method for the synthesis of metal sulfide nanocrystals.

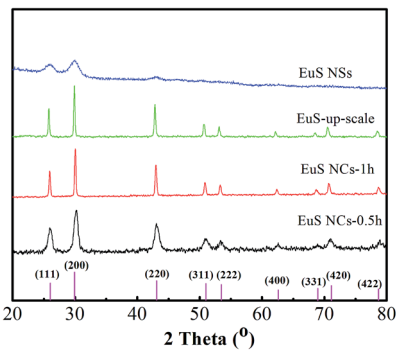

Fig. 2 X-ray diffraction patterns of prepared EuS samples.

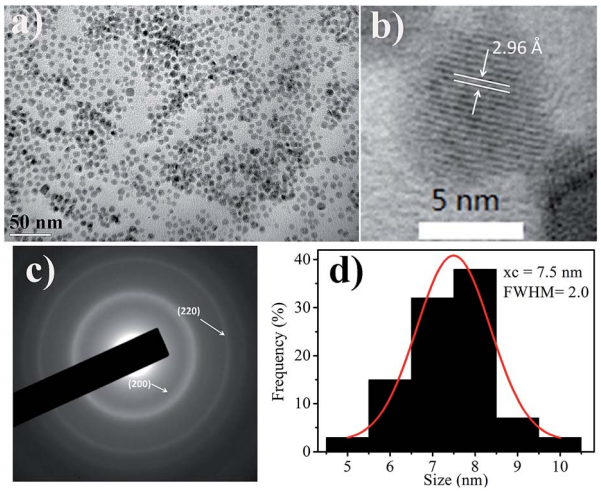

Fig. 3 (a) TEM image of EuS NDs. (b) High resolution TEM image of EuS NDs. (c) SEAD patterns. (d) The size histogram.

Morphologies and crystal structure of Gd_2O_2S nanocrystals

Using the similar experimental procedure, we undertook the thermal decomposition of $Gd(oleate)_3$ in oleylamine/CS_2. The obtained product was first characterized by XRD, as shown in Fig. 4a. All diffraction peaks are well indexed as the hexagonal Gd_2O_2S phase with reference to the JCPDS file 26-1422. The broad diffraction peaks and weak intensity are mainly due to small size of nanocrystals. The composition of the product was further investigated by XPS. The Gd (4p, 4d), O 1s and S (2p, 2s) peaks in the survey spectrum which are in good agreement with the literature reports of Gd_2O_2S[27,28] indicates the obtained products consists of gadolinium, oxygen and sulfur elements (Fig. 4b). The C 1s peak is also observed, possibly due to the C

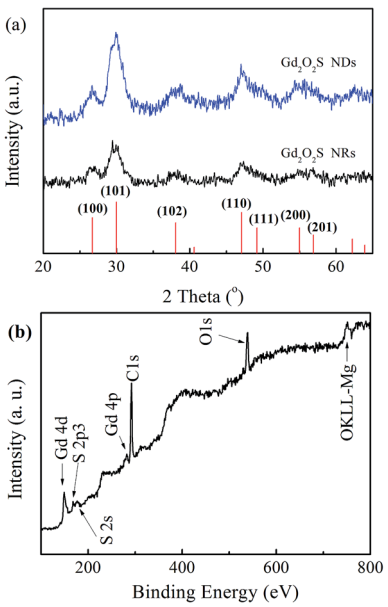

Fig. 4 (a) Powder X-ray diffraction (PXRD) patterns of Gd_2O_2S nanocrystals. (b) XPS spectra of Gd_2O_2S NDs.

contamination of the oleylamine capping at the surface of Gd_2O_2S nanocrystals. The TEM images illustrates that the obtained Gd_2O_2S nanocrystals are nanodots with an average size of ~4.5 nm (Fig. 5a and d). The lattice spacing is 2.98 Å as observed in the high resolution TEM image (Fig. 5b), which corresponds to the distance between the plane (101). The dimensionality of Gd_2O_2S nanocrystals can also be facilely tuned by 1-dodecanethiol as well. In the presence of 1-dodecanethiol, Gd_2O_2S nanorods (NRs) were obtained as shown in Fig. 5e and f. The average diameter of Gd_2O_2S NRs is 2.4 nm (Fig. 5h) and the length-to-width ratio varies from 2.1 to 6.2.

The above XRD, EDX and TEM results prove that Gd_2O_2S nanocrystals were prepared directly from the thermal decomposition of $Gd(oleate)_3$ in oleylamine/CS_2. As mentioned in the Introduction section, it is very difficult to synthesize lanthanide oxysulfides (Ln_2O_2S) through soft synthesis techniques, since the hard Lewis acid Ln^{3+} doesn't preferentially bind to the soft Lewis base S^{2-}.[17] In the previously reported synthesis methods, inconvenient single molecule precursors, high temperature or further sulfuration are needed. The key point in the synthesis of Ln_2O_2S through soft techniques is to find an effective sulfur source. For example, thiourea was used as the sulfur element source to prepare Gd_2O_2S.[29] However the product was amorphous. Because the mixed alcoholic solvents are not good at dissolving H_2S which was released from the decomposition of thiourea at high temperature. The low concentration of S^{2-} ions in this solvothermal reaction system, together with the natural low affinity of S^{2-} with Gd^{3+}, results in the amorphous product. In our suggested method, Gd_2O_2S nanocrystals can be directly obtained in mild experimental conditions, which illustrates that CS_2 is a good sulfur source for the preparation of Ln_2O_2S nanocrystals.

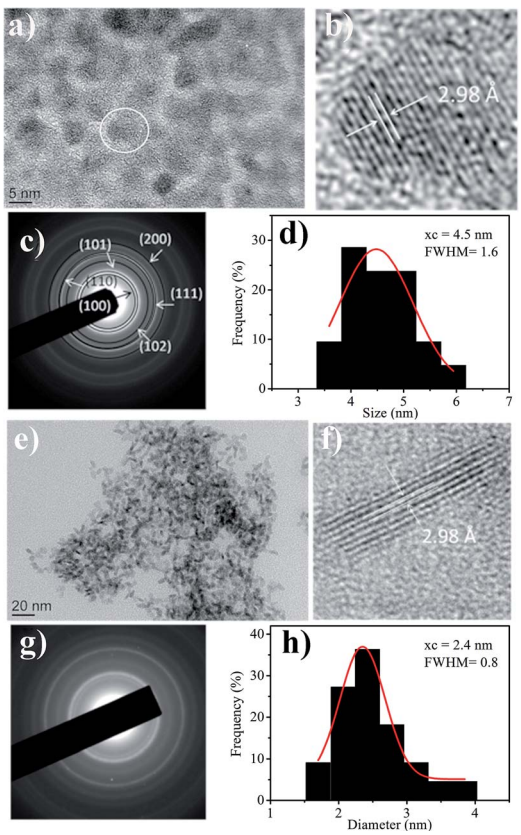

Fig. 5 TEM image of (a) Gd_2O_2S NDs and (e) Gd_2O_2S NRs. (b) and (f) are corresponding high resolution TEM images. (c) and (g) are corresponding SAED patterns. (d) and (h) are corresponding size histograms.

Magnetic properties of EuS and Gd_2O_2S nanocrystals

To investigate the magnetic properties these nanocrystals, the temperature dependence of the magnetizations of these EuS nanocrystals was measured from 300 to 5 K by using Physical Property Measurement System. Fig. 6a gives the curves of reverse magnetic susceptibility χ^{-1} *versus* temperature of EuS NCs and EuS NDs. The Curie temperatures were estimated to be 16.4 K and 16.1 K for EuS NCs and EuS NDs, respectively, through extrapolation from the curves, which agree well with the recognized value 16.6 K of bulk EuS.[30] All magnetic data above 30 K can be well fitted (insets in Fig. 6a) to the Curie–Weiss law:

$$1/\chi = (T - T_C)/C$$

where χ is the magnetic susceptibility, T is the temperature, T_C is the Curie temperature and C is the material-specific Curie constant. As can be clearly seen from Fig. 6a, the EuS NCs has larger Curie constant (or smaller slope) than that of EuS NDs,

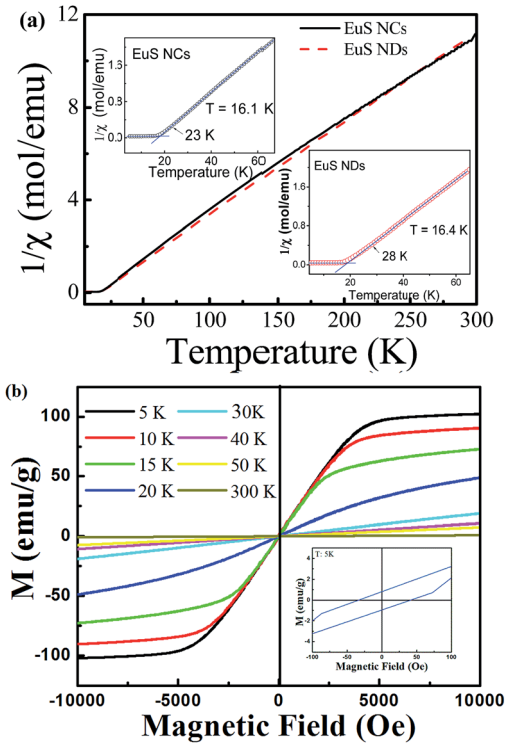

Fig. 6 (a) Temperature dependence of the inverse magnetic susceptibility χ^{-1} of EuS nanocrystals; (b) hysteresis loops of EuS NDs at various temperatures. The inset is the enlarged hysteresis loops of EuS NDs at 5 K.

which can be attributed to the smaller surface/bulk ratio of the EuS NCs.

To further confirm the ferromagnetic property of EuS nanocrystals, we have also carried out temperature dependent M/H measurement. As shown in Fig. 6b for EuS NDs, the magnetic hysteresis loops are obvious below the Curie temperature. In contrast, they disappear above the Curie temperature. When the temperature locates at 5 K, the coercive field (H_c) is about 42 Oe (inset in Fig. 6b), suggesting the magnetic anisotropy in EuS NDs is very small. This is expected as the orbital moment of Eu^{2+} should be zero theoretically.

Fig. 7a shows the curve of magnetic susceptibility χ *versus* temperature of Gd_2O_2S nanocrystals. The magnetic susceptibility of Gd_2O_2S nanocrystals decreases rapidly with the temperature increasing, which indicates the obtained Gd_2O_2S nanocrystals have a paramagnetic property. The inverse susceptibility (H/M) curves (Fig. 7b) show the Curie–Weiss-like behavior of the nanocrystals, which is similar to Gd_2O_3 nanocrystals.[31]

Formation mechanisms

With regards to the possible formation mechanisms of EuS and Gd_2O_2S nanocrystals by using CS_2 as sulfur source, we proposed that CS_2 may react with oleylamine to form dithiocarbamate $[RNH_3^+][RNHCS_2^-]$ firstly,[32] which then reacts with Eu(oleate)$_3$ to give rise to Eu-dithiocarbamate complexes *in situ* (Scheme 1). Under elevated temperature, the complexes were thermally decomposed and Eu^{3+} was reduced to Eu^{2+} by oleylamine, resulting in the formation of EuS nanocubes. 1-dodecanethiol could adsorb on the surface of EuS nuclei through the –SH group and act as a capping ligand, thus suppresses the growth of EuS nanocrystals and lead to the formation of the smaller EuS nanodots. Properly due to the larger standard reduction potential of gadolinium(III) ($E^0_{Gd^{3+}\rightarrow Gd^{2+}} = -3.82$ V) compared to europium(III) ($E^0_{Eu^{3+}\rightarrow Eu^{2+}} = -0.35$ V),[33] Gd^{3+} is much more difficult to be reduced to Gd^{2+} by oleylamine under the same reaction conditions. At the same time, because of the relatively high concentration and activity of S^{2-} in the reaction system, the thermal decompositions of Gd(oleate)$_3$ in oleylamine/CS_2 lead to the formation of Gd_2O_2S NDs. The presence of 1-dodecanethiol could mitigate the growth of Gd_2O_2S crystals, which indicates by the smaller diameters of Gd_2O_2S NRs produced with longer reaction time (10 h) compared with that of Gd_2O_2S NDs. Possibly due to the different adsorption strength of 1-dodecanethiol on the different facets of Gd_2O_2S nuclei, the nuclei slowly grow along a preferential direction, resulting in the formation of nanorods.

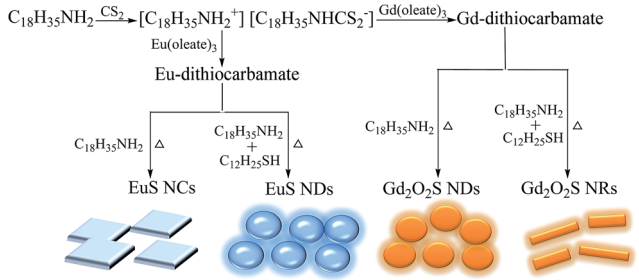

Scheme 1 The suggested formation mechanism of EuS and Gd_2O_2S nanocrystals.

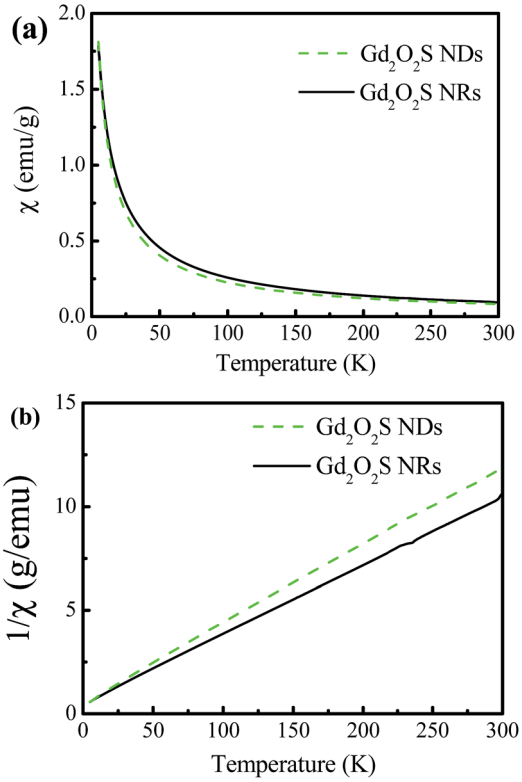

Fig. 7 (a) Temperature dependence of the magnetic susceptibility χ of Gd_2O_2S nanocrystals. (b) Temperature dependence of the inverse magnetic susceptibility χ^{-1} of Gd_2O_2S nanocrystals.

Conclusions

In conclusion, we have developed a facile synthesis method of EuS and Gd_2O_2S nanocrystals by using CS_2 as the sulfur source through the thermal decomposition of Eu(oleate)$_3$ or Gd(oleate)$_3$ in oleylamine, respectively. The obtained EuS and Gd_2O_2S nanocrystals with narrow size distribution illustrate CS_2 is an effective sulfur source for the preparation of metal sulfide and lanthanide oxysulfides semiconductor nanocrystals. Indeed, monodispersed ZnS, PbS and CdS nanodots have been synthesized in the suggested reaction system, which illustrates the generalization of the suggested reaction system. The dimensionality of EuS and Gd_2O_2S nanocrystals can be facilely tuned by the addition of 1-dodecanethiol as a surfactant. The magnetic measurements suggest that the obtained EuS nanocrystals exhibit strong ferromagnetic properties below the Curie temperature, while Gd_2O_2S nanocrystals are paramagnetic.

Acknowledgements

This work was supported by the 973 Program No. 2014CB921104, the NSF of China (Grant No. 61201071, 61306020) and Program of Shanghai Subject Chief Scientist.

Notes and references

1 B. T. Matthias, R. M. Bozorth and J. H. van Vleck, *Phys. Rev. Lett.*, 1961, **7**, 160–161.
2 T. R. McGuire, B. E. Argyle, M. W. Shafer and J. S. Smart, *Appl. Phys. Lett.*, 1962, **1**, 17–18.
3 T. Nagahama, T. S. Santos and J. S. Moodera, *Phys. Rev. Lett.*, 2007, **99**, 016602.
4 B. Li, G.-X. Miao and J. S. Moodera, *Phys. Rev. B: Condens. Matter Mater. Phys.*, 2013, **88**, 161105.
5 I. N. Goncharenko and I. Mirebeau, *Phys. Rev. Lett.*, 1998, **80**, 1082–1085.
6 X. Wan, J. Dong and S. Y. Savrasov, *Phys. Rev. B: Condens. Matter Mater. Phys.*, 2011, **83**, 205201.
7 W. Söllinger, W. Heiss, R. T. Lechner, K. Rumpf, P. Granitzer, H. Krenn and G. Springholz, *Phys. Rev. B: Condens. Matter Mater. Phys.*, 2010, **81**, 155213.
8 R. J. Gambino, R. R. Ruf, T. R. McGuire and P. Fumagalli, *J. Appl. Phys.*, 1991, **70**, 6386–6388.
9 R. S. Selinsky, J. H. Han, E. A. Morales Pérez, I. A. Guzei and S. Jin, *J. Am. Chem. Soc.*, 2010, **132**, 15997–16005.
10 M. Bruchez Jr, M. Moronne, P. Gin, S. Weiss and A. P. Alivisatos, *Science*, 1998, **281**, 2013–2016.
11 M. Nikl, T. Yanagida, H. Yagi, T. Yanagitani, E. Mihokova and A. Yoshikawa, in *Recent Advances in Ceramic Materials Research*, ed. J. J. R. Rovira and M. S. Rubi, Nova Science Publishers, Inc., 2013, pp. 127–176.
12 Z. Huang, Z. Chen, K. Peng, D. Wang, F. Zhang, W. Zhang and Y. Du, *Phys. Rev. B: Condens. Matter Mater. Phys.*, 2004, **69**, 094420.
13 Y. Ma, Y. Dai, M. Guo, C. Niu, Y. Zhu and B. Huang, *ACS Nano*, 2012, **6**, 1695–1701.
14 M. D. Regulacio, S. Kar, E. Zuniga, G. Wang, N. R. Dollahon, G. T. Yee and S. L. Stoll, *Chem. Mater.*, 2008, **20**, 3368–3376.
15 F. Zhao, H.-L. Sun, G. Su and S. Gao, *Small*, 2006, **2**, 244–248.
16 S. K. Dmitry, S. Suseela, H. Weidong, A. H. Melissa, A. M. Stephen and H. D. James, *Nanotechnology*, 2010, **21**, 415601.
17 R. G. Pearson, *J. Am. Chem. Soc.*, 1963, **85**, 3533–3539.
18 T. Kataoka, Y. Tsukahara, Y. Hasegawa and Y. Wada, *Chem. Commun.*, 2005, 6038–6040.
19 Y. Hasegawa, M. Afzaal, P. O'Brien, Y. Wada and S. Yanagida, *Chem. Commun.*, 2005, 242–243.
20 F. Zhao, H.-L. Sun, S. Gao and G. Su, *J. Mater. Chem.*, 2005, **15**, 4209–4214.
21 Y. Hasegawa, Y. Okada, T. Kataoka, T. Sakata, H. Mori and Y. Wada, *J. Phys. Chem. B*, 2006, **110**, 9008–9011.
22 F. Zhao, M. Yuan, W. Zhang and S. Gao, *J. Am. Chem. Soc.*, 2006, **128**, 11758–11759.
23 T. Xia, W.-h. Cao, X.-x. Luo and Y. Tian, *J. Mater. Res.*, 2005, **20**, 2274–2278.
24 S. A. Osseni, S. Lechevallier, M. Verelst, C. Dujardin, J. Dexpert-Ghys, D. Neumeyer, M. Leclercq, H. Baaziz, D. Cussac, V. Santran and R. Mauricot, *J. Mater. Chem.*, 2011, **21**, 18365–18372.
25 D. S. Koktysh, S. Somarajan, W. He, M. A. Harrison, S. A. McGill and J. H. Dickerson, *Nanotechnology*, 2010, **21**, 415601.
26 E. Hemmer, Y. Kohl, V. Colquhoun, H. Thielecke, K. Soga and S. Mathur, *J. Phys. Chem. B*, 2010, **114**, 4358–4365.
27 J. Thirumalai, R. Chandramohan and T. A. Vijayan, *J. Mater. Sci.: Mater. Electron.*, 2011, **22**, 936–943.
28 J. Thirumalai, R. Chandramohan, S. Valanarasu, T. A. Vijayan, R. M. Somasundaram, T. Mahalingam and S. R. Srikumar, *J. Mater. Sci.*, 2009, **44**, 3889–3899.
29 Y. Song, H. You, Y. Huang, M. Yang, Y. Zheng, L. Zhang and N. Guo, *Inorg. Chem.*, 2010, **49**, 11499–11504.
30 D. D. Berkner, *Phys. Lett. A*, 1975, **54**, 396–398.
31 M.-A. Fortin, R. M. Petoral Jr, F. Soederlind, A. Klasson, M. Engstroem, T. Veres, P.-O. Kaell and K. Uvdal, *Nanotechnology*, 2007, **18**, 395501.
32 E. Alper and W. Bouhamra, *Chem. Eng. Technol.*, 1994, **17**, 138–140.
33 L. R. Morss, *Chem. Rev.*, 1976, **76**, 827–842.

